Title

COSMIC REIONIZATION AFTER PLANCK: COULD QUASARS DO IT ALL?

Journal

The Astrophysical Journal Letters, 813(1)

ISSN

2041-8205

Authors

Madau, Piero

Haardt, Francesco

Publication Date

2015-11-01

DOI

10.1088/2041-8205/813/1/l8

Peer reviewed

Preprint typeset using LaTeX style emulateapj v. 5/2/11

COSMIC REIONIZATION AFTER PLANCK: COULD QUASARS DO IT ALL?

Piero Madau[1] and Francesco Haardt[2,3]
[1] Department of Astronomy & Astrophysics, University of California, 1156 High Street, Santa Cruz, CA 95064, USA
[2] Dipartimento di Scienza e Alta Tecnologia, Università dell'Insubria, via Valleggio 11, 22100 Como, Italy
[3] INFN, Sezione Milano/Bicocca, P.za della Scienza 3, 20126 Milano, Italy

ABSTRACT

We assess a model of late cosmic reionization in which the ionizing background radiation arises entirely from high redshift quasars and other active galactic nuclei (AGNs). The low optical depth to Thomson scattering reported by the Planck Collaboration pushes the redshift of instantaneous reionization down to $z = 8.8^{+1.7}_{-1.4}$ and greatly reduces the need for significant Lyman-continuum emission at very early times. We show that, if recent claims of a numerous population of faint AGNs at $z = 4 - 6$ are upheld, and the high inferred AGN comoving emissivity at these epochs persists to higher, $z \gtrsim 10$, redshifts, then active galaxies may drive the reionization of hydrogen and helium with little contribution from normal star-forming galaxies. We discuss an AGN-dominated scenario that satisfies a number of observational constraints: the H I photoionization rate is relatively flat over the range $2 < z < 5$, hydrogen gets fully reionized by $z \simeq 5.7$, and the integrated Thomson scattering optical depth is $\tau \simeq 0.056$, in agreement with measurements based on the Lyα opacity of the intergalactic medium (IGM) and cosmic microwave background (CMB) polarization. It is a prediction of the model that helium gets doubly reionized before redshift 4, the heat input from helium reionization dominates the thermal balance of the IGM after hydrogen reionization, and $z > 5$ AGNs provide a significant fraction of the unresolved X-ray background at 2 keV. Singly- and doubly-ionized helium contribute about 13% to τ, and the He III volume fraction is already 50% when hydrogen becomes fully reionized.

Subject headings: cosmology: theory — dark ages, reionization, first stars — diffuse radiation — intergalactic medium — galaxies: active

1. INTRODUCTION

The reionization of the all-pervading IGM marks a turning point in the history of structure formation in the universe. The details of this process reflect the nature of the first astrophysical sources of radiation and heating as well as the early thermodynamics of cosmic baryons, and continue to be the subject of considerable observational and theoretical efforts (for a recent review, see Robertson et al. 2010). Studies of resonant absorption in the spectra of distant quasars show that, while inhomogeneous hydrogen reionization may still be ongoing at $z \sim 6$, it has fully completed by redshift 5 (e.g., Becker et al. 2015; McGreer et al. 2015; Fan et al. 2006). It is generally agreed that the IGM is kept ionized by the integrated UV emission from active nuclei and star-forming galaxies, but there is still no consensus on the relative contributions of these sources as a function of epoch. The high ionization threshold (4 ryd) and small photoionization cross section of He II, the rapid recombination rate of He III, and the fact that most hot stars lack 4 ryd emission, all delay the double ionization of helium. This is expected to be completed by hard UV-emitting quasars and other AGNs around the apparent peak of their activity at $z \approx 2.5$ (e.g., McQuinn et al. 2009; Haardt & Madau 2012), later than the reionization of H I and He I. It is the traditional view that, at $z > 3$, as the declining population of optically bright quasars makes an increasingly small contribution to the 1 ryd radiation background (e.g. Shapiro & Giroux 1987), massive stars in early galactic halos take over and provide the additional ionizing flux needed (e.g., Madau et al. 1999; Meiksin 2005; Faucher-Giguère et al. 2009).

While plausible, this "two-components" picture for cosmic reionization is not necessarily correct, and warrants further investigation for validation. In particular, star-forming galaxies at $z > 5$ can keep the Universe substantially ionized only if one extrapolates the steep UV luminosity function well below the observed limits and assumes a globally-averaged absolute escape fraction of Lyman-continuum (LyC) radiation into the early IGM, $\bar{f}_{\rm esc}$, that exceeds 20% (e.g., Bouwens et al. 2012; Finkelstein et al. 2012; Haardt & Madau 2012). Such leakage values are higher than typically inferred from observations of luminous galaxies at $z \sim 3 - 4$ once contamination by foreground low-redshift interlopers is accounted for (Vanzella et al. 2012). Despite significant efforts and the examination of hundreds of galaxies, there exists only a handful of robust detections as of today (e.g., Siana et al. 2015; Mostardi et al. 2015).

The Planck Collaboration (2015) has reported a new, smaller value, $\tau = 0.066 \pm 0.016$ of the integrated reionization optical depth from low-multipoles polarization, lensing, and high-multipole temperature CMB data. This corresponds to a sudden reionization event at $z = 8.8^{+1.7}_{-1.4}$ and reduces the need for a large LyC background at very early times. Together with the recent claim by Giallongo et al. (2015) (see also Glikman et al. 2011) of a significant population of faint AGNs at $4 < z < 6.5$, these facts have prompted us to reassess a scenario in which quasars and active galaxies may actually dominate the cosmic reionization process at all epochs, with normal star-forming galaxies making only a negligible contribution due to their small leakages.

We explore this intriguing possibility below, assuming a $(\Omega_M, \Omega_\Lambda, \Omega_b) = (0.3, 0.7, 0.045)$ flat cosmology throughout with $H_0 = 70\ \mathrm{km\,s^{-1}\,Mpc^{-1}}$.

2. QSO COMOVING EMISSIVITY

Figure 1 shows the inferrred quasar/AGN comoving emissivity at 1 ryd as a function of redshift. Our modeling is based on a limited number of contemporary, optically-selected AGN samples (see also Khaire & Srianand 2015 for a similar compilation). All the surveys cited below provide best-fit luminosity function (LF) parameters, which are then used to integrate the LF down to the same relative limiting luminosity, $L_{\rm min}/L_\star = 0.01$. Most of these LFs have faint-end slopes > -1.7, which makes the corresponding volume emissivities rather insensitive to the value of the adopted limiting luminosity. Schulze et al. (2009) combined the Sloan Digital Sky Survey (SDSS) and the Hamburg/ESO survey results into a single $z = 0$ AGN LF covering 4 orders of magnitude in luminosity. In the redshift range $0.68 < z < 3.0$, the g-band LF of Palanque-Delabrouille et al. (2013) combines SDSS-III and Multiple Mirror Telescope quasar data with the 2SLAQ sample of Croom et al. (2009). The $1 < z < 4$ AGN LF by Bongiorno et al. (2007) again merges SDSS data at the bright end with a faint AGN sample from the VIMOS-VLT Deep Survey. The high-redshift quasar LF in the Cosmic Evolution Survey (COSMOS) in the bins $3.1 < z < 3.5$ and $3.5 < z < 5$ has been investigated by Masters et al. (2012), who find a decrease in the space density of faint quasars by roughly a factor of four from redshift 3 to 4. A significantly higher number of faint AGNs at $z \sim 4$ is found by Glikman et al. (2011) in the NOAO Deep Wide-Field Survey and the Deep Lens Survey, and by Giallongo et al. (2015) at $z = 4 - 6$ in the CANDELS GOODS-South field. A novel detection criterion is adopted in Giallongo et al. (2015), whereby high-redshift galaxies are first selected in the NIR H band using photometric redshifts, and become AGN candidates if detected in X-rays by *Chandra*. AGN candidates are found to have X-ray luminosities and rest-frame UV/X-ray luminosity ratios that are typical of Seyfert-like and brighter active nuclei. If correct, these claims suggest that AGNs may be a more significant contributor to the ionizing background radiation than previously estimated.

We have converted the integrated optical emissivity inferred from these studies, ϵ_λ (in units of $\mathrm{erg\,s^{-1}\,Mpc^{-3}\,Hz^{-1}}$), into a 1 ryd emissivity, ϵ_{912}, using a power-law spectral energy distribution, $\epsilon_{912} = \epsilon_\lambda(\lambda/912)^{-\alpha_{\rm uv}}\,\bar{f}_{\rm esc}$, with $\alpha_{\rm uv} = 0.61$ following Lusso et al. (2015). We assume an escape fraction of hydrogen-ionizing radiation $\bar{f}_{\rm esc} = 1$. To assess whether a faint AGN population can dominate the cosmic reionization process under reasonable physical assumptions, we adopt in the following an AGN comoving emissivity of the form

$$\log \epsilon_{912}(z) = 25.15e^{-0.0026z} - 1.5e^{-1.3z}, \qquad (1)$$

for $z < z_{\rm QSO}$, and zero otherwise. Despite the significant scatter in the data points, this function fits reasonably well the $z = 0$, $z < 2.5$, and $4 < z < 5$ emissivities from Schulze et al. (2009), Bongiorno et al. (2007), and Giallongo et al. (2015), respectively. Note that this emissivity does not drop at high redshift like, e.g., the LyC emissivity of luminous quasars inferred by Hopkins et al. (2007) (see Fig. 1). It is also higher compared to previous estimates at low redshift, a fact that could contribute to solve the "photon underproduction crisis" of Kollmeier et al. (2014) (see also Khaire & Srianand 2015).

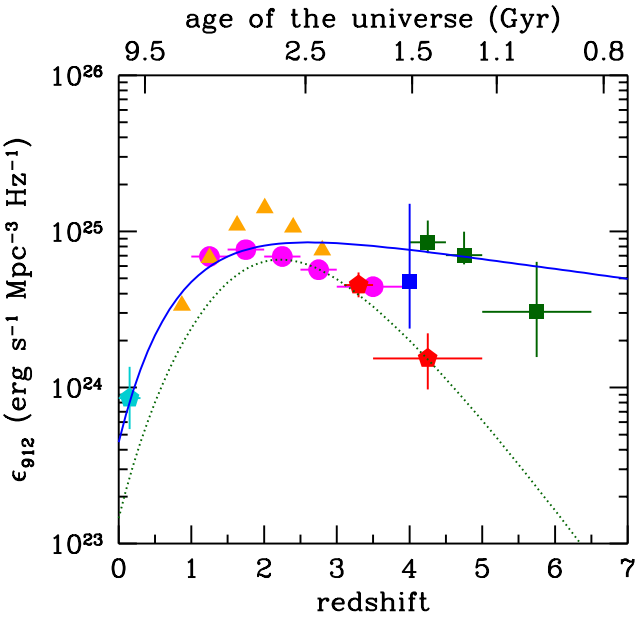

FIG. 1.— The AGN comoving ionizing emissivity inferred from Schulze et al. (2009) (cyan pentagon), Palanque-Delabrouille et al. (2013) (orange triangles), Bongiorno et al. (2007) (magenta circles), Masters et al. (2012) (red pentagons), Glikman et al. (2011) (blue square), and Giallongo et al. (2015) (green squares). The solid curve shows the functional form given in Equation (1). The LyC AGN emissivity of Hopkins et al. (2007) is shown for comparison (dotted line). See text for details.

3. REIONIZATION HISTORY

Reionization is achieved when ionizing sources have radiated at least one LyC photon per atom, and the rate of LyC photon production is sufficient to balance radiative recombinations. Specifically, the time-dependent ionization state of the IGM can be modeled semi-analytically by integrating the "reionization equations" (Madau et al. 1999; Shapiro & Giroux 1987)

$$\frac{dQ_{\rm HII}}{dt} = \frac{\dot{n}_{\rm ion,H}}{\langle n_{\rm H}\rangle} - \frac{Q_{\rm HII}}{t_{\rm rec,H}} \qquad (2)$$

$$\frac{dQ_{\rm HeIII}}{dt} = \frac{\dot{n}_{\rm ion,He}}{\langle n_{\rm He}\rangle} - \frac{Q_{\rm HeIII}}{t_{\rm rec,He}} \qquad (3)$$

for the volume fractions Q of ionized hydrogen and doubly-ionized helium. Here, the angle brackets denote a volume average, gas densities are expressed in comoving units, $t_{\rm rec}$ is a characteristic recombination timescale, and $\dot{n}_{\rm ion} = \int d\nu(\epsilon_\nu/h\nu)$ is the injection rate density of ionizing radiation, i.e. photons between 1 and 4 ryd in the case of H I ($\dot{n}_{\rm ion,H}$) and above 4 ryd for He II ($\dot{n}_{\rm ion,He}$). We do not explicitly follow the transition from neutral to singly-ionized helium, as this occurs nearly simultaneously to and cannot be readily decoupled from the reionization of hydrogen.

The ODEs above assume that the mean free path of UV radiation is always much smaller than the horizon and that the absorption of photons above 4 ryd is dominated by He II. Because only a negligible amount of recombinations occurs in mostly neutral gas, these equations do not explicitly account for the presence of optically thick absorbers that reduce the mean free path of LyC radiation and may further delay reionization (Bolton et al. 2009). They allow, mathematically, for values of Q that are > 1, which is physically impossible.

Following the results of cosmological hydrodynamical simulations by Shull et al. (2012) (see also Finlator et al. 2012), we define the characteristic hydrogen recombination timescale as

$$t_{\rm rec,H} = [(1+\chi)\langle n_{\rm H}\rangle(1+z)^3\langle\alpha_B(T)\rangle\, C_{\rm RR}]^{-1}, \quad (4)$$

where α_B is the case-B radiative recombination rate coefficient, $\chi \equiv Y/[4(1-Y)] = 0.083$ allows for the presence of photoelectrons from He II (here Y is the primordial helium mass fraction), and $C_{\rm RR} = 2.9[(1+z)/6]^{-1.1}$ is the clumping factor of ionized hydrogen that accounts for both density and temperature effects on the average recombination rate. Similarly, the recombination timescale of doubly ionized helium is

$$t_{\rm rec,He} = [(1+2\chi)\langle n_{\rm H}\rangle(1+z)^3 Z\langle\alpha_B(T/Z^2)\rangle\, C_{\rm RR}]^{-1}, \quad (5)$$

where $Z = 2$ is the ionic charge and we have assumed that H II and He III have similar clumping factors. We have numerically integrated the reionization equations from $z_{\rm QSO} = 12$ onwards, extrapolating the AGN emissivity in Equation (1) to $z_{\rm QSO}$, and assuming an EUV power-law spectrum $\propto \nu^{-\alpha_{\rm euv}}$ with $\alpha_{\rm euv} = 1.7$ (Lusso et al. 2015) and a gas temperature of $T = 20,000\,{\rm K}$. The integrated electron scattering optical depth can be calculated as

$$\tau(z) = c\sigma_T\langle n_{\rm H}\rangle \int_0^z \frac{(1+z')^2 dz'}{H(z')}[Q_{\rm HII}(1+\chi) + \chi Q_{\rm HeIII}], \quad (6)$$

where c is the speed of light, σ_T the Thomson cross section, $H(z)$ is the Hubble parameter, and we assumed $Q_{\rm HeII} = Q_{\rm HII} - Q_{\rm HeIII}$.

Figure 2 shows the resulting ionization history, quantified by $Q_{\rm HII}$, $Q_{\rm HeIII}$, and $\tau(z)$. The shading shows the effects of changing clumping factor [$C_{\rm RR} = 9.25 - 7.21\log(1+z)$, Finlator et al. 2012], IGM temperature ($T = 15,000\,{\rm K}$), and EUV spectral slope ($\alpha_{\rm euv} = 1.57$, Telfer et al. 2002; Stevans et al. 2014). With our default parameters, *hydrogen reionization is completed by* $z \simeq 5.7$*, helium is doubly ionized by* $z \simeq 4.2$*, and the Thomson scattering optical depth is* $\tau \simeq 0.056$. The last is consistent with the value reported by the Planck collaboration at the 1σ level. The first agrees with an updated analysis by Becker et al. (2015) of the line-of-sight variance in the intergalactic Lyα opacity at $4 < z < 6$, showing that the data near $z = 5.6 - 5.8$ require fluctuations in the volume-weighted hydrogen neutral fraction that are higher than expected from density variations alone. These fluctuations are most likely driven by large-scale variations in the mean free path, a signature of the trailing edge of the cosmic reionization epoch. As shown in Figure 2, our reionization history is also consistent with the dark pixel fraction observed in the Lyα and Lyβ forest of $z > 6$ quasars, which provides a model-independent upper limit of $1 - Q_{\rm HII} < 0.11$ at $z = 5.9$ (McGreer et al. 2015).

The redshift-dependent fraction of color-selected galaxies revealing Lyα emission has become a valuable constraint on the evolving neutrality of the early IGM. We notice here that, in our late reionization model, the hydrogen neutral fraction evolves quite rapidly from redshift 6 ($1 - Q_{\rm HII} = 0.15$) to redshift 8 ($1 - Q_{\rm HII} = 0.65$). This will cause a fast decline of the mean Lyα line transmissivity of the IGM and may explain the swift drop observed in the space density of Lyα emitting galaxies at $z > 6$ (e.g., Choudhury et al. 2015; Schenker et al. 2014).

While a late hydrogen reionization epoch is not a unique feature of an AGN-dominated scenario, the early reionization of He II is. Traditionally, the peak in luminous quasar activity observed at $z \approx 2.5$ has been expected to coincide with the end of helium reionization. And while observations of patchy absorption in the He II Lyα forest at these epochs have been interpreted as signaling the tail end of He II reionization at $z \leq 2.7$ (e.g., Shull et al. 2010, and references therein), the large fluctuations in the background radiation field above 4 ryd predicted from the rarity of bright quasars and the relatively short attenuation lengths of EUV photons make the interpretation of the He II data still controversial. Indeed, rather than complete Gunn-Peterson absorption at higher redshifts, recent observations have revelead high-transmission regions out to $z = 3.5$ (Worseck et al. 2015), in conflict with numerical models of He II reionization driven by luminous quasars (McQuinn et al. 2009; Compostella et al. 2013). According to Worseck et al. (2015), the observed mild evolution with redshift of He II absorption demands that the bulk of intergalactic helium was already doubly ionized at $z > 3.5$ by a population of early EUV sources. The high AGN comoving emissivity present at $z > 4$ in our model may accomplish just that. We find that singly- and doubly-ionized helium contribute about 13% to τ, and the He III fraction is already 50% when hydrogen becomes fully reionized at redshift 5.7.

4. DISCUSSION

Only the most luminous distant quasars can be detected in surveys such as the SDSS, leaving the contribution of faint AGNs to the early ionizing background highly uncertain. Recent multiwavelength deep surveys have suggested the presence of a hitherto unknown population of faint AGNs (Fiore et al. 2012; Giallongo et al. 2015) and have prompted a reexamination of the role played by AGNs in the reionization of the IGM. We have expanded on previous studies and assessed a model in which the UV radiation responsible for the reionization of hydrogen and helium in the universe arises entirely from quasars and active galaxies. We have assumed here that normal star-forming galaxies will make only a negligible contribution to the AGN LyC emissivity given in Equation (1), which is true provided their globally-averaged escape fraction does not exceed a few percent or so (e.g., Madau & Dickinson 2014).

Compared to the standard picture widely discussed in the literature, the AGN-dominated scenario examined in this work completes hydrogen reionization late ($z \lesssim 6$), double helium reionization early ($z \gtrsim 4$), and produces

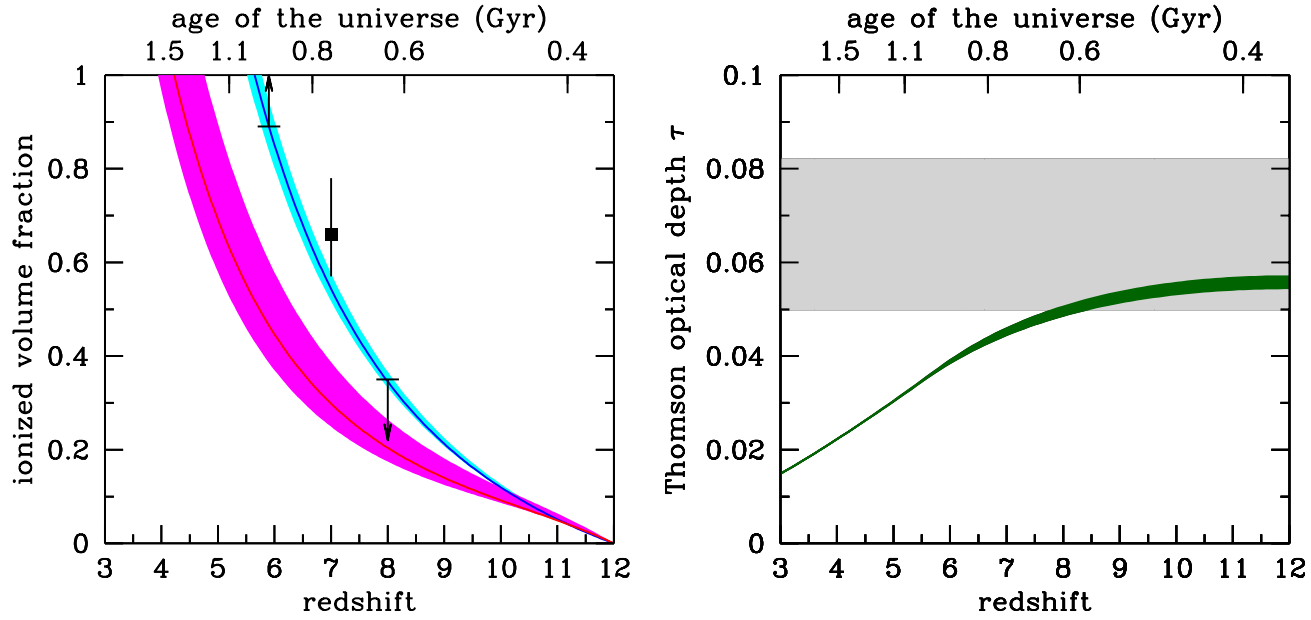

FIG. 2.— Reionization history for our AGN-dominated scenario. Left panel: evolving H II (blue) and He III (magenta) ionized volume fractions for our AGN-dominated scenario. Hydrogen in the IGM is fully reionized when $Q_{\rm HII} = 1$, while helium is doubly reionized when $Q_{\rm HeIII} = 1$. The solid lines correspond to our default model parameters, while the shading shows the effects of changing clumping factor, IGM temperature, and EUV spectral slope (see text for details). Note the "non-standard" early reionization of helium, $Q_{\rm HeIII} = 1$ at $z \gtrsim 4$. The data point at $z = 7$ and the upper limit at $z = 8$ show the constraint on the neutral hydrogen fraction of the IGM inferred from the redshift-dependent prevalence of Lyα emission in the UV spectra of $z = 6 - 8$ galaxies (Schenker et al. 2014). The 1σ lower limit at $z = 5.9$ shows the bound on the neutral hydrogen fraction of the IGM inferred from the dark pixel statistics (McGreer et al. 2015). Right panel: Thomson optical depth to electron scattering, τ, integrated over redshift from the present day (green curve). The Planck constraint $\tau = 0.066 \pm 0.016$ is shown as the gray area.

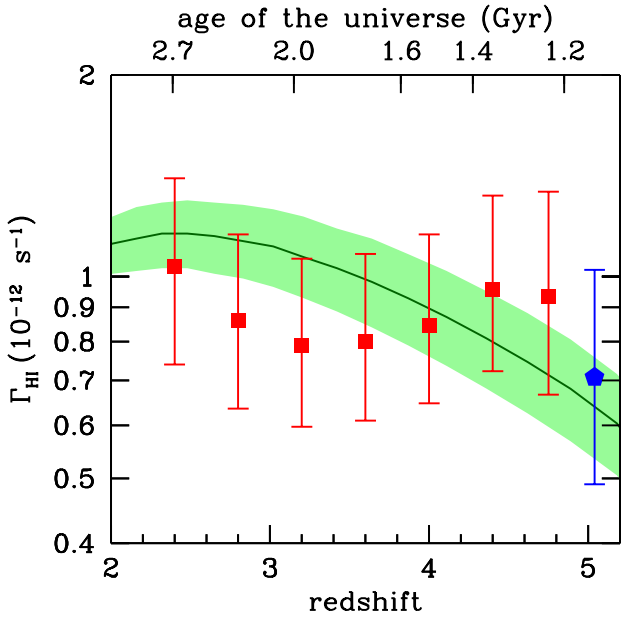

FIG. 3.— The hydrogen photoionization rate, $\Gamma_{\rm HI}$, from $z = 2$ to $z = 5$. The green solid line corresponds to our default AGN-dominated model, while the shading shows the effects of changing the IGM mean free path to ionizing radiation by ±25 percent. Red squares: empirical measurements from the Lyα forest effective opacity by Becker & Bolton (2013). Blue pentagon: same using the quasar proximity effect (Calverley et al. 2011).

a low electron scattering optical depth that is consistent with the Planck value at the 1σ level. It may provide an explanation to some otherwise puzzling recent findings, from the rapid decline of the space density of Lyα emitting galaxies observed at $z > 6$, to an IGM whose temperature is found to increase from redshift 5 to 2 and where He II appears to be predominantly ionized at $z \simeq 3.5$. It is, of course, a model that is also plagued by a number of uncertanties regarding the properties of faint AGNs (their space densities and EUV spectra at high-z), and of the early IGM (its temperature and clumpiness). As already pointed out by Giallongo et al. (2015), a critical assumption is the high escape fraction of ionizing radiation needed for the global AGN population to dominate reionization. While no discernible continuum edge at 912 Å is seen in a composite FUV spectrum of 159 $0 < z < 1.5$ quasars and active galaxies obtained with the Cosmic Origins Spectrograph (COS) (Stevans et al. 2014), it is uncler whether escape fractions of order unity are also typical of fainter, higher redshift AGNs. The model is also somewhat sensitive to $z_{\rm QSO}$, the "formation epoch" of the earliest AGNs. Here, we have assumed $z_{\rm QSO} = 12$ and a comoving AGN emissivity that is only a factor of 3 smaller at $z_{\rm QSO}$ than at redshift 4. In a model with $z_{\rm QSO} = 9$, for example, hydrogen reionization would only be completed by $z \simeq 5.4$.

As a corroboration of the slowly evolving LyC emissivity adopted in this work, we have run a modified version of our radiative transfer code CUBA (Haardt & Madau 2012) to estimate the intensity and spectrum of the filtered ionizing background – specifically the hydrogen photoionization rate $\Gamma_{\rm HI}$ – predicted by our AGN-

dominated scenario,

$$\Gamma_{\rm HI} \equiv \int_{\nu_{\rm HI}}^{\infty} d\nu \, \frac{4\pi J_\nu}{h\nu} \sigma_{\rm HI}(\nu). \quad (7)$$

Here, J_ν is the angle-averaged monochromatic intensity, h is the Planck constant, and $\sigma_{\rm HI}$ and $\nu_{\rm HI}$ are the hydrogen photoionization cross section and ionizing threshold frequency. We have computed the background ionizing intensity J using the emissivity in Equation (1), a EUV spectrum with $\alpha_{\rm euv} = 1.7$, and a new a piecewise parameterization of the distribution in redshift and column density of intergalactic absorbers that fits the measurements of the mean free path of 1 ryd photons by Worseck et al. (2014). The results, shown in Figure 3, are in formal agreement with empirical determinations of $\Gamma_{\rm HI}$ in the interval $2 < z < 5$ based on the Lyα opacity of the IGM (Becker & Bolton 2013). Note that, in the traditional view, the slowly evolving emissivity needed to reproduce the Lyα opacity data can only be achieved by carefully tuning the escape fraction from star-forming galaxies to increase rapidly with lookback time, so as to compensate for the decline in the star formation activity towards early epochs (e.g., Haardt & Madau 2012; Kuhlen & Faucher-Giguère 2012).

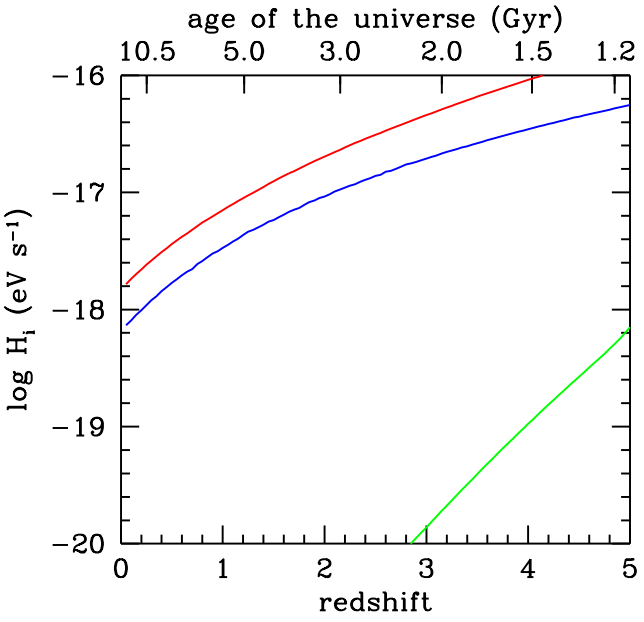

FIG. 4.— Photoheating rates for H I (blue curve), He I (green curve), and He II (red curve) in our AGN-dominated model, from the present epoch to $z = 5$, i.e. after the reionization of hydrogen. All photoheating rates are expressed per hydrogen atom in units of eV s^{-1}, and are computed for gas at the mean cosmic density.

In our AGN-dominated scenario, the heat input from helium reionization will start dominating the thermal balance of the IGM earlier than in the standard picture. In Figure 4 we plot the photoheating rates after the reionization of hydrogen for gas at the mean density,

$$H_i = \langle n_i/n_{\rm H} \rangle \int_{\nu_i}^{\infty} J_\nu \sigma_i (h\nu - h\nu_i) d\nu/(h\nu), \quad (8)$$

for species $i =$ H I, He I, or He II. Here, σ_i and ν_i are the photoionization cross section and threshold frequency for the respective species, and n_i is their abundance (computed integrating the non-equilibrium rate equations for gas at the mean density). The formula above should provide the correct mean heating rate of intergalactic gas once the background intensity J_ν is properly reprocessed while propagating through the IGM (Puchwein et al. 2015). He II photoheating exceeds the hydrogen term by nearly a factor of three. Measurements of the IGM temperature evolution from redshift 5 to 2 derived from the Lyα forest have been known to be inconsistent with the mononotic decrease with redshift expected after the completion of hydrogen reionization (Becker et al. 2011). This discrepancy may be solved by the additional heating provided by an earlier and more extended period of He II reionization.

The population of faint, high redshift AGNs invoked here should leave an imprint on the cosmic X-ray background (XRB). Moretti et al. (2012) derived a value of $J_{2\,\rm keV} \simeq 2.9^{+1.6}_{-1.3} \times 10^{-27}$ erg cm^{-2} s^{-1} Hz^{-1} sr^{-1} to the 2 keV unresolved XRB. The expected contribution at 2 keV from AGNs above redshift z_x can be estimated as (Haardt & Salvaterra 2015)

$$J_{2\,\rm keV} = \frac{c}{4\pi} \int_{z_x}^{\infty} \frac{dz}{(1+z)H(z)} \epsilon_{2\,\rm keV}(z)(1+z)^{-\alpha_x}, \quad (9)$$

where the specific comoving emissivity at 2 keV is related to the LyC emissivity by

$$\epsilon_{2\,\rm keV}(z) = \epsilon_{912}(z) \times R_{\rm II} \left(\frac{2500}{912}\right)^{\alpha_{\rm uv}} \left(\frac{2\,\rm keV}{2500\,\text{Å}}\right)^{-\alpha_{\rm ox}}. \quad (10)$$

Here, $\alpha_{\rm ox}$ is the optical-to-X-ray spectral index needed to join the emissivity at 2500 Å with that at 2 keV, and $R_{\rm II}$ is a correction factor that accounts for the possible contribution of UV obscured ("Type II") AGNs at $z \geq z_x$ to the observed XRB. Using $\alpha_{\rm uv} = 0.61$ as before, $\alpha_{\rm ox} = 1.37$ (Lusso et al. 2010), $\alpha_x = 0.9$, $z_x = 5$, and $R_{\rm II} = 2$ (Merloni et al. 2014) we obtain $J_{2\,\rm keV} = 1.64 \times 10^{-27}$ erg cm^{-2} s^{-1} Hz^{-1} sr^{-1}, i.e. a contribution of nearly 60% to the unresolved XRB. We find that $z > 5$ active galaxies can reionize the universe without overproducing the unresolved XRB provided their properties (i.e. fraction of obscured objects, optical-to-X-ray spectral indices) are similar to those of their lower redshift counterparts (cf. Haardt & Salvaterra 2015; Dijkstra et al. 2004).

Finally, we conclude by pointing out that, in order to promote further testing of this model against new and old observations, we will make the results of our radiative transfer calculations of an AGN-dominated UV background freely available for public use at `http://www.ucolick.org/~pmadau/CUBA`.

We thank E. Giallongo. Z. Haiman, E. Lusso, and A. Meiksin for helpful discussions on various aspects of this paper. P.M. acknowledges support by the NSF through grant AST-1229745 and NASA through grant NNX12AF87G.

REFERENCES

Becker, G. D., & Bolton, J. S. 2013, MNRAS, 436, 1023
Becker, G. D., Bolton, J. S., Haehnelt, M. G., & Sargent, W. L. W. 2011, MNRAS, 410, 1096
Becker, G. D., Bolton, J. S., Madau, P., et al. 2015, MNRAS, 447, 3402
Bolton, J. S., Oh, S. P., & Furlanetto, S. R. 2009, MNRAS, 395, 736
Bongiorno, A., Zamorani, G., Gavignaud, I., et al. 2007, A&A 472, 443
Bouwens, R. J., Illingworth, G. D., Oesch, P. A., et al. 2012, ApJL, 752, L5
Calverley, A. P., Becker, G. D., Haehnelt, M. G., & Bolton, J. S. 2011, MNRAS, 412, 2543
Choudhury, T. R., Puchwein, E., Haehnelt, M. G., & Bolton, J. S. 2015, MNRAS, 452, 261
Compostella, M., Cantalupo, S., & Porciani, C. 2013, MNRAS, 435, 3169
Croom, S. M., Richards, G. T., Shanks, T., et al. 2009, MNRAS, 399, 1755
Dijkstra, M., Haiman, Z., & Loeb, A. 2004, 613, 646
Fan, X., Strauss, M. A., Becker, R. H., et al. 2006, AJ, 132, 117
Faucher-Giguère, C.-A., Lidz, A., Zaldarriaga, M., & Hernquist, L. 2009, ApJ, 703, 1416
Finkelstein, S. L., Papovich, C., Ryan, R. E., et al. 2012, ApJ, 758, 93
Finlator, K., Oh, S. P., Özel, F., & Davé, R. 2012, MNRAS, 427, 2464
Fiore, F., Puccetti, S., Grazian, A., et al. 2012, A&A, 537, A16
Giallongo, E., Grazian, A., Fiore, F., et al. 2015, A&A 578, A83
Glikman, E., Djorgovski, S. G., Stern, D. et al. 2011, ApJL, 728, L26
Haardt, F., & Madau, P. 2012, ApJ, 746, 125
Haardt, F., & Salvaterra, R. 2015, A&A, 575, L16
Hopkins, P. F., Richards, G. T., & Hernquist, L. 2007, ApJ, 654, 731
Khaire, V., & Srianand, R. 2015, MNRAS, 451, L30
Kollmeier, J. A., Weinberg, D. H., Oppenheimer, B. D., et al. 2014, ApJL, 789, L32
Kuhlen, M., & Faucher-Giguère, C.-A. 2012, MNRAS, 423, 862
Lusso, E., Comastri, A., Vignali, C., et al. 2010, A&A, 512, A34
Lusso, E., Worseck, G., Hennawi, J. F., et al. 2015, MNRAS, 449, 4204
Madau, P., & Dickinson, M. 2014, ARA&A, 52, 415
Madau, P., Haardt, F., & Rees, M. J. 1999, ApJ, 514, 648
Masters, D., Capak, P., Salvato, M., et al. 2012, 755, 169
McGreer, I. D., Mesinger, A., & D'Odorico, V. 2015, MNRAS, 447, 499
McQuinn, M., Lidz, A., Zaldarriaga, M., et al. 2009, ApJ, 694, 842
Meiksin, A. 2005, MNRAS, 356, 596
Merloni, A., Bongiorno, A., Brusa, M., et al. 2014, MNRAS, 437, 3550
Moretti, A., Vattakunnel, S., Tozzi, P., et al. 2012, A&A, 548, A87
Mostardi, R. E., Shapley, A. E., Steidel, C. C., et al. 2015, ApJ, 810, 107
Palanque-Delabrouille, N., Magneville, Ch., Yèche, Ch., et al. 2013, A&A, 551, A29
Planck Collaboration 2015, submitted to A&A (arXiv:1502.01589)
Puchwein, E., Bolton, J. S., Haehnelt, M. G., et al. 2015, MNRAS, 450, 4081
Robertson, B. E., Ellis, R. S., Dunlop, J. S., et al. 2010, Nature 468, 49
Schenker, M. A., Ellis, R. S., Konidaris, N. P., & Stark, D. P. 2014, ApJ, 795, 20
Schulze, A., Wisotzki, L., & Husemann, B. 2009, A&A 507, 781
Shapiro, P. R., & Giroux, M. L. 1987, ApJL, 321, L107
Shull, J. M., France, K., Danforth, C. W., et al. 2010, ApJ, 722, 1312
Shull, J. M., Smith, B. D., & Danforth, C. W. 2012, ApJ, 759, 23
Siana, B., Shapley, A. E., Kulas, K. R., et al. 2015, ApJ, 804, 17
Stevans, M. L., Shull, J. M., Danforth, C. W., & Tilton, E. M. 2014, ApJ, 794, 75
Telfer, R. C., Zheng, W., Kriss, G. A., & Davidsen, A. F. 2002, ApJ, 565, 773
Vanzella, E., Guo, Y., Giavalisco, M., et al. 2012, ApJ, 751, 70
Worseck, G., Prochaska, J. X., Hennawi, J. F., & McQuinn, M. 2015, ApJ, submitted (arXiv:1405.7405)
Worseck, G., Prochaska, J. X., O'Meara, John M., et al. 2014, MNRAS, 445, 1745